$= 1.0 \times 10^5\ M^{-1}$, a result in reasonable agreement when one considers the approximate nature of the Debye-Hückel equation under these conditions.

Concentration effects have been shown to play an important part in quenching efficiency when donors and acceptors are simultaneously bound to DNA, as is the case here at low salt concentration.[16] On the other hand, drug mobility on the one-dimensional surface[10] is unlikely to be of significance in these systems since the rate of deintercalation of NiT4 is orders of magnitude slower than rates of migration of ZnT4 along the DNA helix.[14] If mobility were a determining factor, then NiT4 would show much lower quenching efficiencies than ZnT4. Rather, an important aspect of the role played by the DNA becomes apparent from the distance dependence inherent in the region of influence model proposed here to account for the quenching results. For the usual dipole coupling (Förster) mechanism the efficiency of quenching follows an inverse sixth power dependence on distance between donor and quencher. However, a previous study has shown that this predicted dependence is not observed for fluorophores bound to oligonucleotides and that drug-DNA electronic interactions may be important.[35] These same researchers point out that the data of an earlier report[36] indicate that the efficiency of energy transfer from oligonucleotide-bound excited fluorescein to rhodamine is virtually unchanged whether the two dyes are separated by *four or eight base pairs*. Rapid drop-off of efficiency as predicted by the Förster mechanism occurs only at longer distances. Although admittedly in a highly simplified way, the step function of the region of influence model presented here shows a similar distance profile.

The sphere of action model upon which the present approach is based has been applied to a few solution systems as, for example, oxygen quenching of perylene.[30] In general, the sphere radius measured is only slightly larger than the sum of the fluorophore and quencher radii and it is concluded that the two species must be nearly in contact for quenching to occur.[37] This is in marked contrast to the results obtained here. We believe the results of this study point out that, in agreement with the findings of Cooper and Hagerman[35] and Cardullo et al.,[36] an important influence of the DNA matrix is to permit extensive electronic communication between bound drug molecules—an influence that serves to raise the efficiency of transition dipole coupling at long distances. Electronic communication of this type can contribute in part to properties as diverse as the unusual spectral features of DNA-bound chromophores (e.g., large bathochromic shifts are sometimes observed that cannot be simulated with mono- or dinucleotides)[13,15,38] and drug synergism. We are currently proceeding with studies to consider the role base specificity, porphyrin basicity, and metal redox properties play in this communication process.

Acknowledgment. We express our appreciation to the Monsanto Corp., the Pew Charitable Trust, the Henry and Camille Dreyfus Foundation, and the National Science Foundation (Grant CHEM-8915264) for their support of this work.

(35) Cooper, J. P.; Hagerman, P. J. *Biochemistry* **1990**, *29*, 9261.
(36) Cardullo, R. A.; Agrawal, S.; Flores, C.; Zamecnik, P. C.; Wolf, D. E. *Proc. Natl. Acad. Sci.* **1988**, *85*, 8790.
(37) Lakowicz, J. R. *Ibid.* 273.
(38) Pasternack, R. F.; Gibbs, E. J.; Antebi, A.; Bassner, S.; De Poy, L.; Turner, D. H.; Williams, A.; La Place, F.; Lansard, M. H.; Merienne, C.; Perrée-Fauvet, M.; Gaudemer, A. *J. Am. Chem. Soc.* **1985**, *107*, 8179.

Properties of the Excited-Singlet States of Bacteriochlorophyll *a* and Bacteriopheophytin *a* in Polar Solvents

Michael Becker,† V. Nagarajan, and William W. Parson*

Contribution from the Department of Biochemistry, University of Washington, Seattle, Washington 98195. *Received December 3, 1990. Revised Manuscript Received May 6, 1991*

Abstract: Several approaches were used to characterize the lowest excited-singlet states of bacteriochlorophyll *a* (BChl-*a*) and bacteriopheophytin *a* (BPh-*a*). Fluorescence quantum yields for BChl-*a* measured in five polar solvents ranged from 11% in methanol to 20% in pyridine; BPh-*a* had a fluorescence yield of 8% in methanol and 10% in acetone. In each solvent, the emission spectrum did not show mirror symmetry with the absorption spectrum: the fluorescence spectrum was narrower, and its vibrational shoulder was less pronounced and occurred at shorter wavelengths than predicted from the absorption spectrum. The apparent temperature of the excited state, as calculated by the Stepanov relationship, was higher than the ambient temperature (296 K) by about 30 K. The anomalous fluorescence properties can be explained qualitatively by inhomogeneous broadening and vibronic mixing in the excited state. In spite of these anomalies, the fluorescence yields are close to the yields calculated on the basis of previously measured fluorescence lifetimes (Connolly, J. S.; Samuel, E. B.; Janzen, A. F. *Photochem. Photobiol.* **1982**, *36*, 565-574) and calculated radiative lifetimes, indicating that the overall vibrational partition functions are similar in the ground and excited states. Picosecond transient absorption spectra were measured with BChl-*a* in methanol, 1-propanol, and pyridine, using 605-nm excitation pulses with a width of about 0.8 ps. The spectra in the 780-nm region are characterized by a sharp negative trough that shifts to the red with time. The shifting probably reflects adjustments of the stimulated-emission spectrum in response to dielectric relaxation of the solvent around the excited molecule. The relaxation in pyridine is well described by a single exponential with a time constant of 2.7 ± 0.1 ps. The shifting in the alcohols can be fit by biexponentials with time constants of 1.5 ± 0.2 and 18 ± 3 ps in methanol, and 1.1 ± 0.4 and 82 ± 25 ps in 1-propanol. By using an actinometric method to determine the number of molecules in the excited state, the absorption changes at long delay times were used to calculate the $S_{1\rightarrow n}$ absorption spectrum of the thermally equilibrated excited state. The broad, featureless spectrum has an absorption cross section $\sigma_{1\rightarrow n}$ of $(1.0 \pm 0.2) \times 10^{-16}$ cm^2 at 750 nm.

Bacteriochlorophyll (BChl, Figure 1) is a Mg tetrahydroporphyrin that functions both to capture photons and to transfer electrons in photosynthetic bacteria. Figure 1 shows the absorption spectrum of BChl-*a* in pyridine. The four absorption bands can be described in terms of electronic transitions among the two highest filled molecular orbitals and two normally unoccupied orbitals.[1] The strong absorption band near 770 nm, termed the

† Present address: Strukturforschung, Max-Planck Institut für Biochemie, W-8033, Martinsried bei München, Germany.

0002-7863/91/1513-6840$02.50/0

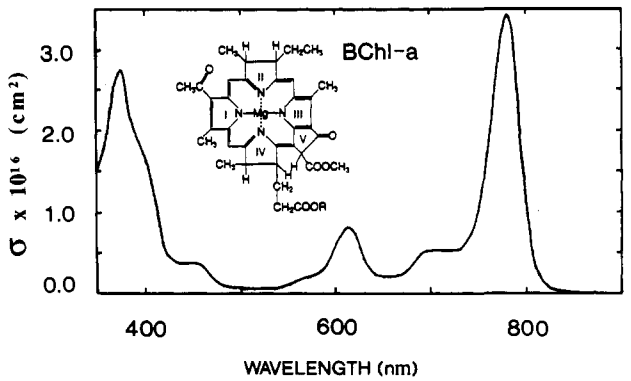

Figure 1. Absorption spectrum of BChl-*a* in pyridine. Insert: structure of BChl-*a*. The BChl-*a* isolated from *Rhodospirillum rubrum* has a geranylgeranyl side chain (R); that from some other bacterial species has a phytyl group.

"Q_y" band, has a transition dipole oriented approximately along the axis connecting the nitrogens of rings I and III. The weaker "Q_x" transition in the region of 600 nm is polarized approximately along the perpendicular axis connecting rings II and IV. Two overlapping, higher energy transitions contribute absorption peaks near 390 and 360 nm. Bacteriopheophytin (BPh), which contains two protons in place of the Mg atom, has corresponding absorption bands in the regions of 750, 525, 380, and 355 nm.

The properties of the lowest excited-singlet state of BChl underlie the electron-transfer processes that occur in the reaction center (RC) of photosynthetic bacteria. The RC is a pigment–protein complex that contains a closely interacting dimer of BChls, along with two additional molecules of BChl and two BPhs. When the BChl dimer is raised to an excited singlet state, it transfers an electron to one of the BPhs in about 3.5 ps, possibly by way of an intervening BChl.[2] Photosynthetic bacteria also contain BChl–protein complexes that serve to absorb light and pass energy to the RC by resonance energy transfer.

Considering the importance of BChl in photosynthesis, there is surprisingly little information on the properties of BChl in its excited singlet states. However, Connolly et al.[3] have measured the fluorescence lifetime τ_f of BChl-*a* and BPh-*a* in a variety of solvents. The lifetimes ranged from 2.3 to 3.6 ns, depending on the solvent. Fluorescence quantum yields were not measured directly, but were calculated with the expression

$$\Phi_f = \tau_f/\tau_0 \tag{1}$$

Here τ_0 is the radiative lifetime, which Connolly et al.[3] estimated from the absorption and emission spectra by the method of Strickler and Berg.[4] The calculated fluorescence yields ranged from 12% to 26%, being lowest in alcohols. In aprotic solvents, the calculated yield depended on whether the Mg bound one or two solvent molecules as axial ligands. More recently, Losev et al.[5] measured fluorescence yields and lifetimes for BChl-*a* in several solvents. The reported yields that were systematically lower than those calculated by Connolly et al. Losev et al. examined only one alcoholic solvent, methanol, but found that the fluorescence yield in it was not significantly different from the yields in aprotic solvents.

In the present study, we have measured fluorescence quantum yields of BChl-*a* and BPh-*a* with the objective of examining the calculated values of τ_0 that underlie the use of eq 1. A critical exploration of such calculations for BChl seemed needed because calculated values of τ_0 for the BChl dimer have been used in analyses of the free energy changes that accompany the initial electron-transfer reactions in the RC.[6]

The Strickler–Berg[4] expression for τ_0 can be written

$$1/\tau_0 = 8\pi cn^2\left[\frac{Q_g}{Q_e}\right]\langle\tilde{\nu}_f^{-3}\rangle^{-1}\int\sigma(\tilde{\nu})\tilde{\nu}^{-1}\,d\tilde{\nu} \tag{2}$$

Here c is the speed of light; n is the refractive index of the solvent; Q_g and Q_e are the vibrational partition functions of the ground and excited states, each defined relative to the lowest vibrational level of the state; $\langle\tilde{\nu}_f^{-3}\rangle = \int F(\tilde{\nu})\tilde{\nu}^{-3}\,d\tilde{\nu}/\int F(\tilde{\nu})\,d\tilde{\nu}$, where $F(\tilde{\nu})$ is the fluorescence amplitude (in units of relative photons·s^{-1}/cm^{-1}) at wavenumber $\tilde{\nu}$ (cm^{-1}); and $\sigma(\tilde{\nu})$ is the absorption cross section (cm^2) at $\tilde{\nu}$. The Strickler–Berg equation was derived for strongly allowed electronic transitions in which there is little change in nuclear structure. The term Q_g/Q_e was not included in the original derivation[4] and was not used by Connolly et al.,[3] but was shown by Ross[7] to be needed.

Ross[7] also has derived the more general expression

$$1/\tau_0 = 8\pi c\tilde{\nu}_m^2 n^2\left[\frac{Q_g}{Q_e}\right]\left[\frac{\sigma(\tilde{\nu}_m)}{F(\tilde{\nu}_m)}\right]e^{|\tilde{\nu}_0-\tilde{\nu}_m|/k_BT}\int F(\tilde{\nu})\,d\tilde{\nu} \tag{3}$$

where $\tilde{\nu}_m$ is any wavenumber at which both F and σ can be measured, and $\tilde{\nu}_0$ is the 0–0 transition energy; k_B is the Boltzmann constant, and T is the temperature. Equation 2 can be derived from this expression if the absorption and emission spectra obey the mirror-symmetry relationship.[7] If we choose $\tilde{\nu}_m = \tilde{\nu}_0$, eq 3 simplifies to

$$1/\tau_0 = 8\pi c\tilde{\nu}_0^2 n^2\left[\frac{Q_g}{Q_e}\right]\left[\frac{\sigma_0}{F_0}\right]\int F(\tilde{\nu})\,d\tilde{\nu} \tag{4}$$

where σ_0 and F_0 are the absorption cross section and fluorescence at $\tilde{\nu}_0$. Equations 3 and 4 make no assumptions about changes in nuclear structure, but, like eq 2, they do assume that the vibrational sublevels of the excited state are thermally equilibrated.

The partition-function ratio that enters into eq 2–4 (Q_g/Q_e) is often assumed, either explicitly or implicitly, to be unity. Although the resulting values of τ_0 frequently prove accurate for calculating fluorescence yields, there also are numerous cases in which the calculated yields disagree with experiment.[7,8] Ross[7] suggested that some of these discrepancies reflect changes in the partition function. In a harmonic system, for example, the vibrational partition function for electronic state s is given by

$$Q_s = \prod_u\sum_{q=1}^{\infty}\exp[-q\tilde{\nu}_u/k_BT] = \prod_u\{1-\exp[-\tilde{\nu}_u/k_BT]\}^{-1} \tag{5}$$

where $\tilde{\nu}_u$ is the wavenumber of vibrational mode u. The ratio Q_g/Q_e could deviate from unity if nuclear distortions associated with excitation cause the vibrational frequencies in the excited state to differ from those of the ground state.

Ross[7] noted that changes in the vibrational partition function can be evaluated by writing

$$Q_g/Q_e = \tau_0^{calc}/\tau_0^{exp} \tag{6}$$

Here τ_0^{calc} is the radiative lifetime calculated by eq 2 or 3 without taking the factor Q_g/Q_e into account, and τ_0^{exp} is the

(1) (a) Gouterman, M. *J. Mol. Spectrosc.* **1961**, *6*, 138–163. (b) Weiss, C. *J. Mol. Spectrosc.* **1972**, *44*, 37–80. (c) Petke, J. D.; Maggiora, J. M.; Shipman, L. L.; Christoffersen, R. E. *Photochem. Photobiol.* **1980**, *32*, 399–414.

(2) (a) Woodbury, N. W.; Becker, M.; Middendorf, D.; Parson, W. W. *Biochemistry* **1985**, *24*, 7516–7521. (b) Breton, J.; Martin, J.-L.; Migus, A.; Antonetti, A.; Orszag, A. *Proc. Natl. Acad. Sci. U.S.A* **1986**, *83*, 5121–5125. (c) Holzapfel, W.; Finkele, U.; Kaiser, W.; Oesterhelt, D.; Scheer, H.; Stilz, H. U.; Zinth, W. *Proc. Natl. Acad. Sci. U.S.A.* **1990**, *87*, 5168–5172. (d) Kirmaier, C.; Holten, D. *Proc. Natl. Acad. Sci. U.S.A.* **1990**, *87*, 3552–3556. (e) Nagarajan, V.; Parson, W. W.; Gaul, D.; Schenck, C. C. *Proc. Natl. Acad. Sci. U.S.A.* **1990**, *87*, 7888–7892.

(3) Connolly, J. S.; Samuel, E. B.; Janzen, A. F. *Photochem. Photobiol.* **1982**, *36*, 565–574.

(4) Strickler, S. J.; Berg, R. A. *J. Chem. Phys.* **1962**, *37*, 814–822.

(5) Losev, A. P.; Sagun, E. I.; Kochubeev, G. A.; Nichiporovich, I. N. *J. Appl. Spectrosc. (USSR)* **1986**, *45*, 798–803.

(6) (a) Arata, H.; Parson, W. W. *Biochim. Biophys. Acta* **1981**, *638*, 201–209. (b) Woodbury, N. W.; Parson, W. W. *Biochim. Biophys. Acta* **1984**, *767*, 345–361.

(7) Ross, R. T. *Photochem. Photobiol.* **1975**, *21*, 401–406.

(8) (a) Birks, J. B.; Dyson, D. J. *Proc. R. Soc. London* **1963**, *A275*, 135–148. (b) Birks, J. B. *Photophysics of Aromatic Molecules*; Wiley-Interscience: New York, 1970; pp 85–87.

"experimental" radiative lifetime obtained from eq 1 with experimentally measured fluorescence lifetimes and quantum yields. We have followed this approach to calculate Q_g/Q_e ratios for BChl-*a* and BPh-*a*.

Another way to determine whether substantial changes in nuclear structure accompany the formation of the excited state is to compare the shapes of the absorption and emission spectra, after weighting the spectra according to the mirror-symmetry relationship:[8]

$$\frac{F(\tilde{\nu})}{\tilde{\nu}^3} \propto \frac{\sigma(2\tilde{\nu}_0 - \tilde{\nu})}{2\tilde{\nu}_0 - \tilde{\nu}} \tag{7}$$

This relationship assumes that $B_{g,u\rightarrow e,\nu} \approx B_{e,u\rightarrow g,\nu}$, where $B_{g,u\rightarrow e,\nu}$ is the Einstein coefficient for an absorptive transition from vibrational level u of the ground electronic state to level ν of the excited state, and $B_{e,u\rightarrow g,\nu}$ is the Einstein coefficient for induced emission from vibrational level u of the excited state to level ν of the ground state. A departure from mirror symmetry suggests that the ground and excited states have different nuclear configurations, and often is associated with a breakdown of eq 2.[8]

Equations 2–4, 6, and 7 all assume that the fluorescence occurs from a thermally equilibrated state, in which the vibrational sublevels are populated according to a Boltzmann distribution. This assumption can be examined by determining whether the emission spectrum is related to the absorption spectrum in conformance with the Stepanov expression:[9]

$$\ln [F(\tilde{\nu})/\tilde{\nu}^2\sigma(\tilde{\nu})] \propto -\tilde{\nu}/k_BT^* \tag{8}$$

where T^* is the apparent temperature of the excited state. The proportionality constant here can be obtained by combining eq 1 and 3 and dropping the subscript m:

$$\ln\left(\frac{[\Phi_f/\tau_f]\ F(\tilde{\nu})/\int F(\tilde{\nu})\,d\tilde{\nu}}{8\pi cn^2\tilde{\nu}^2\sigma(\tilde{\nu})}\right) = -\tilde{\nu}/k_BT^* + \tilde{\nu}_0/k_BT^* + \ln(Q_g/Q_e) \tag{9}$$

(An expression that was essentially the same as eq 9 except for the omission of n and the term $\ln(Q_g/Q_e)$ was derived by Neporent.[9b]) If spontaneous emission occurs from a homogeneous system in a thermally equilibrated state, a plot of the function on the left-hand side of eq 8 or 9 versus $\tilde{\nu}$ should be a straight line with a slope of $-1/k_BT^*$, and T^* should equal the ambient temperature. Because deviations from this relationship have been observed for other molecules, including chlorophyll-*a*,[10] we have assessed its applicability to BChl and BPh.

Picosecond laser spectroscopy provides a way to examine the dynamics of thermal equilibration of excited molecules more directly. In the second section of the studies described here, we use picosecond absorption spectroscopy to investigate the relaxations of excited BChl-*a* in solution. To evaluate the importance of the solvent in the relations, measurements were made in pyridine, methanol (MeOH), and 1-propanol (1-PrOH). The relaxation dynamics are particularly relevant to an understanding of how nuclear relaxations bear on the electron-transfer kinetics in the RC. We also have determined the absorption and stimulated-emission spectra of the lowest excited-singlet state of BChl-*a* in MeOH, with the aim of aiding the interpretation of the transient spectroscopic signals seen in RCs and BChl antenna complexes.

A preliminary account of some of this work has been presented.[11]

Materials and Methods

Materials. BChl-*a* was purified from *Rhodospirillum rubrum* S-1 as described,[12a] and was stored in pyridine in the dark at −5 °C. Prior to each experiment, the pyridine was evaporated under O_2-free nitrogen, and the pigment was redissolved in the solvent of interest. BPh-*a* was produced from BChl-*a* by evaporation of the pyridine, addition of a few drops of glacial acetic acid, and evaporation of the acid.[12a] All manipulations were done in the dark. HPLC measurements[12b] showed that the BChl samples contained BChl-*a* and BChl-*a'* (the epimer at position 13^2) in a ratio of approximately 5:1. BChl samples kept in pyridine contained less than 1% 13^2-hydroxy-BChl-*a* and 2-desvinyl-2-acetylchlorophyll-*a*, even after prolonged periods at 295 K. Samples allowed to stand in MeOH at 295 K for 8 h (the duration of a typical set of fluorescence or picosecond measurements) contained between 2 and 5% 13^2-hydroxy-BChl-*a* and about 2% 2-desvinyl-2-acetylchlorophyll-*a*.

Rhodamine 101 (also known as rhodamine 640) was obtained from Exciton and was recrystallized from dimethyl sulfoxide to check for impurities. The relative fluorescence yield of the recrystallized dye was indistinguishable from that of the dye as supplied. Reaction centers were purified from *Rhodobacter sphaeroides* R-26 as described,[2a] and were suspended in 10 mM TrisHCl buffer, pH 8.0, 0.1% lauryldimethylamine oxide.

Fluorescence Measurements. Fluorescence quantum yields were measured relative to a standard of known yield, rhodamine 101. Excitation light from a 250-W tungsten–iodine lamp passed through a water filter and a 0.25-m monochromator with a 3-nm bandpass. To minimize self-absorption of the emission, the excitation beam was focused to a narrow vertical band that passed through the sample cuvette along the edge closest to the detector. Fluorescence was detected at 90°, through a 0.2-m monochromator, by a Hamamatsu R632 photomultiplier in a cooled housing. The photomultiplier output was processed by home-built photon-counting electronics. The fluorescence spectra presented here and used in the quantum yield determinations were averages of at least six measurements, and were corrected for the spectral sensitivity of the detection system. The spectral sensitivity was determined by using a tungsten–iodine lamp with a known color temperature (2800 K). For this measurement, a filter was placed in front of the photomultiplier to remove second-order light; corrections were made for the spectrum of the filter.

Solutions of rhodamine 101 in ethanol were excited at 564 nm; bacterial pigments were excited at the peak of their Q_x absorption band in the solvent of interest (see Table I). The ratios of the excitation intensities at the two wavelengths were measured both with a radiometer and by scattering excitation light off a white surface toward the photomultiplier. The peak optical densities of the sample and the dye were ≤0.1 in the long-wavelength absorption band and <0.05 in the Q_x band. (The BChl-*a* concentration was approximately 1 μM). A 2-fold increase in sample or dye concentration did not significantly affect the apparent fluorescence yield of either. The absorption and emission spectra of the samples did not change significantly over the course of the measurements.

The fraction of the emitted light detected in a fluorimeter generally depends quadratically on the refractive index of the solvent.[14] We found that the relative fluorescence yields of rhodamine 101 in ethanol, dimethyl sulfoxide, and pyridine did vary with the square of the refractive index, and fluorescence yields of the bacterial pigments were corrected accordingly. Possible polarization effects were investigated by placing a polarizing filter in the excitation beam and an analyzing filter at 54.7° in the detection path. The fluorescence quantum yield of BChl-*a* in 1-PrOH measured with this arrangement was indistinguishable from the yield measured in the absence of the filters, so polarization filters were not used routinely.

With the correction for the refractive index (n), the fluorescence quantum yield is[15]

$$\Phi_f = \Phi_f^r\left(\frac{n}{n^r}\right)^2\left(\frac{\int F(\lambda)\,d\lambda}{\int F^r(\lambda)\,d\lambda}\right)\left(\frac{I_{ex}^r}{I_{ex}}\right)\left(\frac{1-10^{-A^r_{ex}}}{1-10^{-A_{ex}}}\right) \tag{10}$$

where the superscript "r" refers to the rhodamine reference and terms without a superscript refer to the sample, $F(\lambda)$ is the fluorescence at

(9) (a) Stepanov, B. I. *Dokl. Acad. Nauk SSSR* **1957**, *112*, 839–841; Engl. transl.: *Sov. Phys.-Dokl.* **1957**, *2*, 81–84. (b) Neporent, B. S. *Dokl. Akad. Nauk SSSR* **1958**, *119*, 682–685; Engl. transl.: *Sov. Phys.-Dokl.* **1958**, *3*, 337–340. (c) Ross, R. T. *J. Chem. Phys.* **1967**, *46*, 4590–4593.

(10) (a) Hevesi, J.; Singhal, G. S. *Spectrochim. Acta* **1969**, *25A*, 1751–1758. (b) Singhal, G. S.; Hevesi, J. *Photochem. Photobiol.* **1971**, *14*, 509–514. (c) Szalay, L.; Singhal, G. S.; Tombacz, E.; Kozma, L. *Acta Phys. Acad. Sci. Hung.* **1973**, *34*, 341–350. (e) Van Metter, R. L.; Knox, R. S. *Chem. Phys.* **1976**, *12*, 333–340. (f) Knox, R. S.; Van Metter, R. L. In *Chlorophyll Organization and Energy Transfer in Photosynthesis*; CIBA Foundation Symposium 1979; Vol. 61, pp 177–190.

(11) Becker, M.; Nagarajan, V.; Middendorf, D.; Shield, M. A.; Parson, W. W. In *Current Research in Photosynthesis*; Baltschefsky, M., Ed.; Kluyer: Dordrecht, 1990; pp 101–104.

(12) (a) Scherz, A.; Parson, W. W. *Biochim. Biophys. Acta* **1984**, *766*, 653–665. (b) Struck, A.; Scheer, H. *FEBS Lett.* **1990**, *261*, 385–388.

(13) (a) Evans, T. A.; Katz, J. J. *Biochim. Biophys. Acta* **1975**, *396*, 414–426. (b) Callahan, P. M.; Cotton, T. M. *J. Am. Chem. Soc.* **1987**, *109*, 7001–7007.

(14) Ediger, M. D.; Moog, R. S.; Boxer, S. G.; Fayer, M. D. *Chem. Phys. Lett.* **1982**, *88*, 123–127.

(15) Parker, C. A.; Rees, W. T. *Analyst* **1960**, *85*, 587–599.

wavelength λ (corrected for the wavelength dependence of the detection system), I_{ex} is the intensity of the excitation beam (photons·cm^{-2}·s^{-1}), and A_{ex} is the optical density at the excitation wavelength.

To examine the effect of O_2 on the fluorescence yields, sample and reference solutions were bubbled with O_2-free N_2 for various lengths of time. This had no significant effect on the measured fluorescence yield of BChl-*a* or BPh-*a* in any of the solvents. For rhodamine 101 in ethanol, the fluorescence yield of an un-deoxygenated sample was about 91% of the yield of a sample that had been deoxygenated for one or more hours. The rhodamine solutions therefore were deoxygenated for at least 1 h prior to each experiment. The fluorescence yield of rhodamine 101 in O_2-free ethanol (Φ_f') was taken to be 100%.[16]

The BChl-*a* and BPh-*a* solutions usually had a small fluorescence emission peak at about 690 nm, probably from the contaminant 2-desvinyl-2-acetylchlorophyll-*a*,[17] which could be excited preferentially at 430 nm. With Q_x excitation, the integrated area of the contaminant's emission band was usually <5% of the area of the main emission band of the BChl. Because the overlap of the contaminant's fluorescence with the main fluorescence band was small, a linear interpolation was used to edit out the contaminant band. We evaluated the maximum effect of contaminant absorbance by assuming that all of the absorbance at 680 nm was due to the contaminant and calculating the absorbance at the excitation wavelength using the absorption spectrum of 2-desvinyl-2-acetylchlorophyll-*a*.[17] The calculated effect on the fluorescence yield was insignificant.

Steady-state absorption spectra were measured with a Shimadzu UV-160 spectrophotometer interfaced to a computer. Extinction coefficients for BChl-*a* were taken from Connolly et al.[3] Extinction coefficients for BPh-*a* ($\epsilon_{746.5nm}$ = 37 500 M^{-1} cm^{-1} in MeOH and 47 100 M^{-1} cm^{-1} in acetone) were obtained by converting a known amount of BChl-*a* to BPh-*a*.

Picosecond Experiments. Picosecond difference spectra were measured using a double-beam, pump-probe technique with diode arrays for detection.[2a,2e,18] The cross-correlation width of the excitation and probe pulses was approximately 0.8 ps. Solutions of BChl-*a* in alcohols were flowed continuously from a cooled reservoir through a cuvette with a pathlength of 1 mm. Samples in pyridine were stirred in a cuvette with a pathlength of 2 mm. The absorbances at the Q_y maximum were adjusted to be between 0.8 and 1.3. Varying the absorbance over this range did not alter the shapes of the transient difference spectra. The wavelength of the excitation dye laser was tuned to be near the Q_x peak in each solvent (Table I). Typically, the maximum negative signal (absorbance decrease plus stimulated emission) was about 30% of the maximum absorbance of the Q_y band. Data were collected in time steps of 0.25 ps near the excitation pulse and larger steps at later times. Degradation of the samples during the measurements was negligible, judging from the ground-state absorption spectra. Artifacts due to fluorescence stimulated by the excitation beam were checked by blocking the probe beams and detecting the photons emitted from the excited but unprobed sample, and were found to be negligible. To investigate possible artifacts due to lasing by the BChl samples,[19] the cuvette was tilted away from perpendicular to the probe beams, and the excitation beam was realigned; the shapes of the difference spectra were unaffected.

To characterize the time-dependent shifting of the picosecond difference spectrum, we extracted the maximum amplitude of the difference spectrum at each time point (ΔA_{peak}), along with the wavelength of the peak and the width and skewness of the spectrum, by fitting the spectrum to a log-normal function.[20] Each spectrum was fit over the wavelength region where $|\Delta A|$ exceeded 30% of $|\Delta A_{peak}|$; excellent fits were obtained in all cases. The time-dependent position of the peak then was fit to the convolution of an excitation function $E(t)$ with a single- or double-exponential relaxation:

$$\bar{\nu}_{peak}(t_u) = \sum_{w=1}^{u} E(t_w)\{\sum_{i=1}^{1 \text{ or } 2} \chi_i \exp[-k_i(t_u - t_w)] + \chi_0\} \qquad (11)$$

Here $\bar{\nu}_{peak}(t_u)$ is the peak position at time t_u, χ_i and k_i are the initial amplitude and relaxation rate constant for component i, and χ_0 is a constant. The excitation function is

$$E(t_w) = R(t_w)/\sum_{\nu=1}^{w} R(t_\nu) \qquad (12)$$

where $R(t)$ is an instrument response function that reflects a convolution of the pump and probe pulses. $R(t)$ was obtained by integrating the measured ΔA over the wavelength region from 720 to 830 nm, and differentiating this integral with respect to time:

$$R(t) = \frac{d}{dt}\left(\int_{720}^{830} \Delta A(\lambda,t)\, d\lambda\right) \qquad (13)$$

The sum in the denominator of eq 12 takes into account that fact that $\bar{\nu}_{peak}(t)$ represents an average of all the molecules that have been excited up to time t. The relaxation time constants reported below are averages from two independent experiments in each solvent.

Possible artifacts associated with chirping of the probe pulse were examined with a computer model in which a Gaussian difference spectrum was probed with a linearly chirped pulse and the peak of the distorted spectrum was calculated at various times relative to the excitation. With chirping of about 1 ps per 250 nm, which is characteristic of the apparatus used here, the spectral shifting due to chirping was negligible by 0.5 ps after the center of the excitation pulse. This indicates that the relaxation time constants measured with BChl probably were not distorted greatly by chirping. The relaxations probably were not due to rotational reorientation of the BChl, because they were not affected detectably by changing the excitation pulse polarization from linear to circular.

The picosecond difference spectra contain contributions from bleaching of the ground-state absorption, stimulated emission from the excited state, and excited-state absorption:

$$\Delta A(\lambda) = [\sigma_{1\rightarrow n}(\lambda) - \sigma_{0\rightarrow 1}(\lambda) - \sigma_{1\rightarrow 0}(\lambda)]\kappa d C_{ex}^{BChl} \qquad (14)$$

Here $\sigma_{0\rightarrow 1}(\lambda)$ is the ground-state absorption cross section, $\sigma_{1\rightarrow n}(\lambda)$ is the cross section for absorption by the excited state, $\sigma_{1\rightarrow 0}(\lambda)$ is the stimulated-emission cross section, C_{ex}^{BChl} is the concentration of excited molecules, d is the cuvette pathlength, and κ is a constant that relates the molar extinction coefficient to the absorption cross section (2.63×10^{20} M^{-1} cm). To dissect these different contributions to $\Delta A(\lambda)$, we first evaluated $\sigma_{1\rightarrow 0}(\lambda)$ as follows.

The cross section for stimulated emission at wavenumber $\bar{\nu}$ is related to that at $\bar{\nu}_0$ by the ratio of the spontaneous fluorescence amplitudes at the two wavenumbers:

$$\frac{\sigma_{1\rightarrow 0}(\bar{\nu})}{\sigma_{1\rightarrow 0}(\bar{\nu}_0)} = \left(\frac{\bar{\nu}_0}{\bar{\nu}}\right)^2 \frac{F(\bar{\nu})}{F(\bar{\nu}_0)} \qquad (15)$$

This expression, which reflects the relationship between the Einstein coefficients for stimulated emission and fluorescence, assumes that the population distribution among vibrational states in the picosecond experiment is the same as in the measurement of the spontaneous fluorescence. The calculated value of $\sigma_{1\rightarrow 0}$ therefore applies only after the relaxations considered above. The cross section for stimulated emission at $\bar{\nu}_0$ can be related to the absorption cross section at this wavenumber:

$$\frac{\sigma_{1\rightarrow 0}(\bar{\nu}_0)}{\sigma_{0\rightarrow 1}(\bar{\nu}_0)} \approx \frac{Q_g}{Q_e} \qquad (16)$$

Equation 16 incorporates the identity of the Einstein coefficients for absorption and induced emission between the lowest vibrational levels of the ground and excited states ($B_{g,0\rightarrow e,0} = B_{e,0\rightarrow g,0}$), and uses the partition functions to express the fractions of the molecules that are in these vibrational levels. It is an approximation because part of the absorption and induced emission at $\bar{\nu}_0$ is due to molecules that are in higher vibrational levels. Combining eq 1, 4, 15, and 16 gives

$$\sigma_{1\rightarrow 0}(\lambda) \approx \frac{[\Phi_f/\tau_f]\,\lambda^4 F(\lambda)}{n^2 8\pi c \int F(\lambda)\, d\lambda} \qquad (17)$$

where $F(\lambda)$ is the measured fluorescence in units of relative photons·s^{-1}/nm [$F(\lambda) = \lambda^{-2}F(\bar{\nu})$]. Peterson et al.[21] have derived a similar expression.

Given $\sigma_{0\rightarrow 1}(\lambda)$ and $\sigma_{1\rightarrow 0}(\lambda)$, eq 14 can be solved for $\sigma_{1\rightarrow n}(\lambda)$ if C_{ex}^{BChl} is known. One way to determine C_{ex}^{BChl} would be to saturate the absorbance changes to obtain 100% conversion. The laser flashes used here were not sufficiently intense for this. We therefore used an actinometric method, in which the absorbance changes with BChl were compared to absorbance changes measured with photosynthetic reaction centers (Figure 2). The RC absorption band at 865 nm bleaches instantly and remains bleached over the time scale of the measurements.[2] The change

(16) (a) Drexhage, K. H. In *Dye Lasers* (*Topics in Applied Physics, Vol 1*), Schäfer, F. P., Ed.; Springer-Verlag: Berlin, 1973; pp 144–193. (b) Karstens, T.; Kobs, K. *J. Phys. Chem.* **1980**, *84*, 1871–1872.
(17) Smith, J. R. L.; Calvin, M. *J. Am. Chem. Soc.* **1966**, *88*, 4500–4506.
(18) Becker, M.; Nagarajan, V.; Middendorf, D.; Parson, W. W.; Martin, J. E.; Blankenship, R. E. *Biochim. Biophys. Acta* **1991**, *1057*, 299–312.
(19) Hindman, J. C.; Kugel, R.; Svirmickas, A.; Katz, J. J. *Proc. Natl. Acad. Sci. U.S.A.* **1977**, *74*, 5–9.
(20) Siano, D. B.; Metzler, D. E. *J. Chem. Phys.* **1969**, *51*, 1856–1861.
(21) Peterson, O. G.; Webb, J. P.; McColgin, W. C.; Eberly, J. H. *J. Appl. Phys.* **1971**, *42*, 1917–1928.

Table I. Q_x Absorption Maxima, Fluorescence Yields and Lifetimes, Calculated Radiative Lifetimes, and Calculated Partition-Function Ratios

	solvent	lig.[a]	$\lambda_{max}^{Q_x}$ (nm)	Φ_f	τ_f[b] (ns)	τ_0^{exp} (ns)	τ_0^{calcc} (ns)	τ_0^{calcd} (ns)	Q_g/Q_e[e]	Q_g/Q_e[f]
BChl	pyridine	2	610	0.20 ± 0.01	3.53	18	27.8	13.2	1.5	0.73
	MeOH	2	605	0.11 ± 0.01	2.32	21	28.3	17.6	1.3	0.83
	1-PrOH	2	611	0.14 ± 0.01	2.54	18	19.4	16.9	1.1	0.94
	MeCN	1	579	0.14 ± 0.01	3.08	22	28.8	17.1	1.3	0.78
	acetone	1	578	0.16 ± 0.01	3.14	20	24.2	16.6	1.2	0.83
BPh	MeOH		527	0.08 ± 0.02	2.25	28	40.8	24.2	1.5	0.86
	acetone		524	0.10 ± 0.01	2.55	26	32.7	21.8	1.3	0.84

[a] Number of axial ligands of Mg.[13] [b] From Connolly et al.[3] [c] Calculated by eq 4, using the $\bar{\nu}_0$ values given in Table II and neglecting the term Q_g/Q_e. [d] Calculated by eq 2, neglecting the term Q_g/Q_e. [e] Calculated by eq 6, using τ_0^{calc} from eq 4. [f] Calculated by eq 6, using τ_0^{calc} from eq 2.

in extinction coefficient associated with this bleaching is known ($\Delta\epsilon_{865}^{RC}$ = 1.12×10^5 M^{-1} cm^{-1}).[22] Thus, if the excitation intensity (I_{ex}) is the same for the BChl and RC samples and Beer's law is satisfied,

$$C_{ex}^{BChl} = \frac{\Delta A_{865}^{RC}}{d\Phi_{et}^{RC}\Delta\epsilon_{865}^{RC}}\left(\frac{1 - 10^{-A_{ex}^{BChl}}}{1 - 10^{-A_{ex}^{RC}}}\right) \quad (18)$$

Here A_{ex}^{BChl} and A_{ex}^{RC} are the optical densities of the BChl and RC samples at the excitation wavelength, ΔA_{865}^{RC} is the observed bleaching of the RC sample at 865 nm, and Φ_{et}^{RC} is the quantum yield of electron transfer in the RC. The quantum yield of electron transfer when RCs are excited at 600 nm with continuous illumination is 0.96.[23] Equation 18 assumes that excitation in the Q_x band of BChl provides the S_1 (Q_y) state with 100% yield. It is valid only for very weak excitation flashes, when multiphoton excitations are negligible. Combining eq 14 and 18, and including the requirement for weak excitation, we have

$$\sigma_{1\to n}(\lambda) = \sigma_{0\to 1}(\lambda) + \sigma_{1\to 0}(\lambda) + \Delta A_n(\lambda)\left(\frac{\Delta\epsilon_{865}^{RC}\Phi_{et}^{RC}/\kappa}{\lim_{I_{ex}\to 0}|\Delta A_{865}^{RC}|/|\Delta A_{peak}^{BChl}|}\right)\left(\frac{1 - 10^{-A_{ex}^{RC}}}{1 - 10^{-A_{ex}^{BChl}}}\right) \quad (19)$$

where $\Delta A_n(\lambda)$ is the picosecond difference spectrum for BChl, measured at relatively long times after the excitation flash and normalized to −1 at λ_{peak}.

To compare the picosecond absorbance changes in BChl and RCs as a function of the excitation intensity, a graded neutral density filter was translated through the excitation beam. Measurements were alternated between the BChl and RC samples several times in each experiment. The samples had similar absorbances in the region of 770 to 800 nm. The extrapolation of $|\Delta A_{865}^{RC}|/|\Delta A_{peak}^{BChl}|$ to $I_{ex} = 0$ was carried out by fitting the ratio to a cubic polynomial as illustrated in the inset in Figure 2b. The shape of the transient absorbance spectrum for BChl ($\Delta A_n(\lambda)$) could be measured with relatively strong excitation flashes because it did not change significantly with intensity (data not shown).

Though the laser flashes that we used were not strong enough to saturate the BChl samples (Figure 2a), the absorbance changes measured with RCs did approach saturation (Figure 2b). However, the asymptote (ΔA_{max}) obtained by fitting the RC data to a cumulative, one-hit Poisson saturation curve ($\Delta A = \Delta A_{max}[1 - \exp(-\Phi_{et}^{RC}I)]$, where I is the number of photons absorbed per RC) was only about 50% of the value expected on the basis of the effect of continuous illumination. A similar effect was observed by Moskowitz and Malley,[24] who found that the maximal absorbance change obtained by exciting RCs with saturating, 10-ps pulses at 530 nm was only about 60% of that obtained with saturating continuous light. This effect probably reflects singlet–singlet annihilation in RCs that absorb more than one photon.

Results

Spontaneous Fluorescence. Table I gives the measured quantum yields for BChl-*a* and BPh-*a* in several solvents. Our results for BChl-*a* are identical with those of Losev et al.[5] in two of the three solvents that were studied in common (1-PrOH and acetone). All of the yields are slightly lower than those that Connolly et al.[3] calculated from the fluorescence lifetimes, but the uncertainties in most of the yields overlap. In pyridine, where Connolly et al. obtained 26 ± 2% and Losev et al. reported 16 ± 2%, we found an intermediate value, 20 ± 1%. Of the solvents studied here,

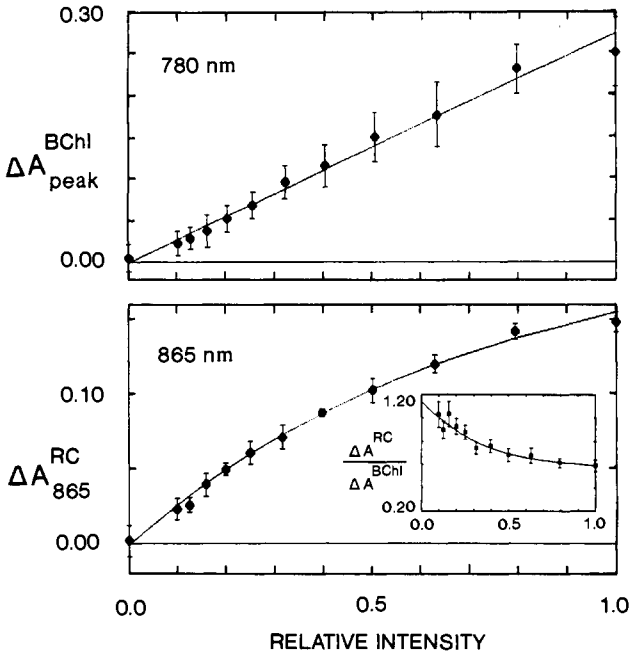

Figure 2. Dependence of the amplitude of the transient absorbance changes on the intensity of the excitation flash for (a) BChl-*a* in pyridine and (b) RCs. The inset in (b) shows the ratio $|\Delta A_{865}^{RC}|/|\Delta A_{peak}^{BChl}|$, with a fit to a cubic polynomial.

alcohols gave the lowest fluorescence yields. Among the aprotic solvents pyridine, acetonitrile, and acetone, the yields were lowest in solvents that provide only a single axial ligand to the Mg of BChl. These trends agree with the results obtained by Connolly et al.[3]

To examine whether BChl-*a* and BPh-*a* obey the mirror-symmetry relationship, we weighted the absorption and emission spectra according to eq 7. Figure 3a shows the expected and observed fluorescence spectra for BChl-*a* in pyridine; Figure 3, b and c, shows similar comparisons for BChl-*a* and BPh-*a* in MeOH. Neither BChl-*a* nor BPh-*a* obeyed the mirror-symmetry relationship closely, and the agreement could not be improved materially by adjusting the symmetry axis, $\bar{\nu}_0$. In all the solvents, the vibrational shoulder of the emission spectrum was lower in amplitude and closer in energy to the main band than expected, and the main band was narrower than predicted. For BChl-*a*, the width of the unweighted emission spectrum at half-height was about two-thirds that of the absorption spectrum (Table II).

Plots of the Stepanov expression (eq 9) are presented in Figure 4, along with the unweighted absorption and fluorescence spectra of BChl-*a* and BPh-*a* in several solvents. The plots are linear over much of the emission band but decrease in slope at low frequencies. Table II gives the T^* values obtained from the slopes in the central regions of the spectra where $F(\bar{\nu})$ is greater than 1/2 maximal. With all of the solvents, T^* is elevated above the ambient temperature (296 K) by about 30 K. Similar fits over only the low-frequency regions of the plots give values that typically are higher by an additional 30 to 60 K. In contrast, rhodamine 101, which exhibited near-perfect mirror symmetry, gave a good fit to eq 9 with T^* = 294 K (data not shown). For comparison, we

(22) Straley, S. C.; Parson, W. W.; Mauzerall, D. C.; Clayton, R. K. *Biochim. Biophys. Acta* **1973**, *305*, 597–609.
(23) Wraight, C. A.; Clayton, R. K. *Biochim. Biophys. Acta* **1973**, *333*, 246–260.
(24) Moskowitz, E.; Malley, M. M. *Photochem. Photobiol.* **1978**, *27*, 55–59.

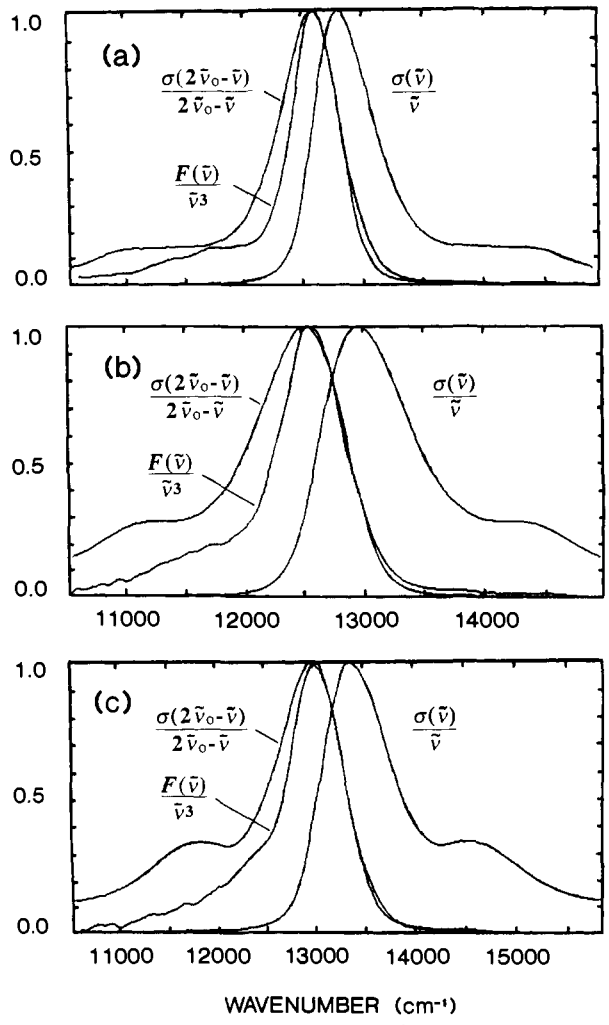

Figure 3. Absorption spectra weighted by $\tilde{\nu}^{-1}$, and smoothed emission spectra weighted by $\tilde{\nu}^{-3}$, for (a) BChl-*a* in pyridine, (b) BChl-*a* in MeOH, and (c) BPh-*a* in MeOH. The spectra are normalized at their peaks. Also shown are the mirror images of the weighted absorption spectra, as given by $\sigma(\tilde{\nu}_0 - \tilde{\nu})/(2\tilde{\nu}_0 - \tilde{\nu})$ (eq 7). The values of $\tilde{\nu}_0$ used here were obtained simply from the intersections of the normalized, weighted absorption, and emission spectra. (The fluorescence spectra were measured in units of photons·s^{-1}/nm and were converted to units of photons·s^{-1}/cm^{-1} by the relationship $F(\tilde{\nu}) = F(\lambda)|d\lambda/d\tilde{\nu}| = F(\lambda)\tilde{\nu}^{-2}$.)

Table II. Q_y Absorption and Emission Maxima, Stokes Shifts, Bandwidths, T^*, and $\tilde{\nu}_0$

	solvent	$\lambda_{max}^{Q_y}$ (nm)	λ_{max}^{fluor} (nm)	Stokes shift (cm^{-1})	W_{abs}[a] (cm^{-1})	W_f[b] (cm^{-1})	T^*[c] (K)	$\tilde{\nu}_0$[c] (cm^{-1})
BChl	pyridine	780.5	792	186	620	494	325	12690
	MeOH	770.5	793	368	974	682	319	12780
	1-PrOH	775.5	795	316	858	633	331	12730
	MeCN	765.5	789	389	939	645	337	12860
	acetone	770.0	786	264	776	583	328	12850
BPh	MeOH	746.5	766	345	897	697	337	12240
	acetone	746.5	763	312	780	602	315	13270

[a] Full width of the Q_y absorption band at half-maximum amplitude. [b] Full width of the emission band at half-maximum amplitude. [c] Obtained with eq 9 by considering only the region of the emission band where $F(\tilde{\nu})$ was greater than half-maximal, and taking Q_g/Q_e to be 1.0.

also excited BChl-*a* in pyridine at 374 nm, thus forcing the excited molecule to dissipate a larger amount of energy. If thermal equilibrium is not attained, T^* should be higher than it is after excitation in the Q_x band. We found a T^* similar to that obtained with Q_x excitation.

Equation 9 can be used to find $\tilde{\nu}_0$, if one knows the value of Q_g/Q_e. As an approximation, we assumed that this ratio is

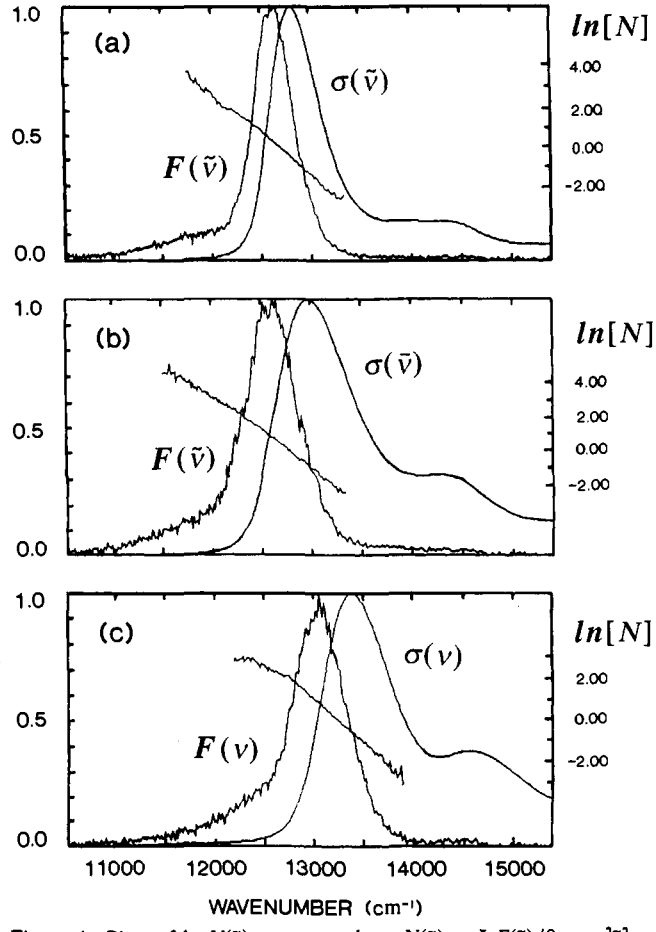

Figure 4. Plots of ln $N(\tilde{\nu})$ versus $\tilde{\nu}$, where $N(\tilde{\nu}) = \Phi_f F(\tilde{\nu})/8\pi c\tau_f n^2\tilde{\nu}^2\sigma(\tilde{\nu})\int F(\tilde{\nu})\,d\tilde{\nu}$ (eq 9) for (a) BChl-*a* in pyridine, (b) BChl-*a* in MeOH, and (c) BPh-*a* in MeOH. Also shown are the unweighted absorption spectra and unsmoothed emission spectra. The spectra are normalized at their peaks.

sufficiently close to unity so that ln $(Q_g/Q_e) \ll \tilde{\nu}_0/k_BT^*$. The resulting values of $\tilde{\nu}_0$ obtained by fitting only the data from the central regions of the emission spectra are given in Table II. For BChl-*a*, the values vary over a range of about 170 cm^{-1} depending on the solvent. Including the vibrational shoulder of the emission spectrum results in a higher value of $\tilde{\nu}_0$.

Table I lists the "experimental" radiative lifetimes (τ_0^{exp}) obtained by eq 1 with our measured values of Φ_f and the values of τ_f measured by Connolly et al.[3] To determine the apparent ratio Q_g/Q_e by eq 6, theoretical radiative lifetimes were calculated from the absorption and emission spectra by both eq 2 and 4. Estimates of the $\tilde{\nu}_0$ values needed in eq 4 were obtained from the plots of eq 9 as just discussed. The radiative lifetimes calculated by the Ross expression (eq 4) are systematically longer than the experimental lifetimes, whereas lifetimes calculated by the Strickler–Berg expression (eq 2) are systematically shorter. Using eq 4 for τ_0^{calc} gives values of Q_g/Q_e that range from 1.1 to 1.5, depending on the solvent; using eq 2 gives results ranging from 0.73 to 0.94. However, the results obtained with eq 4 are very sensitive to the choice of $\tilde{\nu}_0$. With BChl-*a* in MeOH, for example, increasing $\tilde{\nu}_0$ by only about 30 cm^{-1} decreases τ_0^{calc} so that it coincides with τ_0^{exp}, making $Q_g/Q_e = 1.0$.

Picosecond Absorption Changes and Stimulated Emission. BChl in pyridine, MeOH, or 1-PrOH was excited in the Q_x band, and the resulting absorbance changes and stimulated emission were measured in the near-infrared. Figure 5 shows representative spectra for BChl in MeOH. Two features of the spectra are particularly noteworthy: the negative peaks are located to the red of the ground-state Q_y absorption peak (cf. Table II), and the spectra shift further to the red with time.

Figure 6 shows how the position of the peak of the difference spectrum ($\tilde{\nu}_{peak}$) changes with time in the three solvents. The data

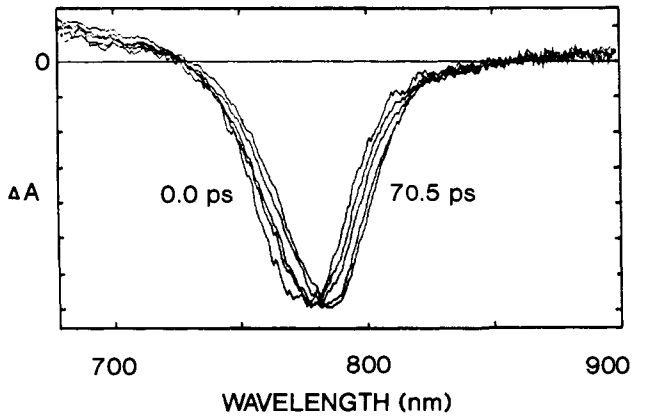

Figure 5. Transient difference spectra of BChl in MeOH, normalized at their negative peaks, measured at (from left to right) 0.0, 1.0, 3.0, 19.5, and 70.5 ps relative to the excitation flash. The amplitudes of the signals at the peaks did not change significantly with time after 1.0 ps.

for BChl in pyridine are fit well by a single-exponential relaxation with a time constant of 2.7 ± 0.1 ps. Double-exponential expressions give satisfactory fits for the alcohols. The time constants are 1.5 ± 0.2 and 18 ± 3 ps in MeOH, and 1.1 ± 0.4 and 82 ± 25 ps in 1-PrOH. The total magnitude of the shift is about two-thirds of the Stokes shift in each of the solvents (cf. Table II).

The contributions of absorbance changes and stimulated emission to the signals at relatively long delay times can be dissected as described in Methods. Figure 7 shows the calculated spectra of stimulated emission and absorption by the excited state of BChl-*a* in MeOH. The $S_{1\rightarrow n}$ absorption spectrum is broad and featureless and has an absorption cross section $\sigma_{1\rightarrow n} = (1.0 \pm 0.2) \times 10^{-16}$ cm^2 at 750 nm and $(0.9 \pm 0.5) \times 10^{-16}$ cm^2 at the peak of the Q_y absorption band (771 nm). The uncertainty in the calculated $\sigma_{1\rightarrow n}$ is greatest slightly to the red of the peak of the Q_y band, where the peaks of the difference spectrum and of the sum of the absorption and stimulated-emission spectra cancel. Figure 7 shows a dip in $\sigma_{1\rightarrow n}$ in this region, but this varied in size in different experiments and could result from an underestimate of the amount of excited BChl or from the approximations underlying eq 17. The stimulated emission occurs in a sharp band near 800 nm, suggesting that the relaxations described above are dominated by shifting of the emission spectrum, rather than by changes in the absorption spectrum of the excited state.

Discussion

Fluorescence Quantum Yields. The measured fluorescence yields of BChl-*a* in polar solvents range from 11 to 20% (Table I). Tait and Holten[25] have reported that the triplet yield for BChl-*a* is approximately 30% in both pyridine and acetonitrile. Combining this number with the fluorescence yields leaves about 50% of the decay of the excited state to occur by internal conversion in pyridine, and 56% in acetonitrile. For BPh-*a*, we measured fluorescence yields of 10% in acetone and 8% in MeOH. Using a measured fluorescence lifetime and a radiative lifetime calculated by the Strickler–Berg expression, Gouterman and Holten[26] calculated a fluorescence yield of 9.4% for BPh in acetone/MeOH (7:3 v/v), in good agreement with the average of the values determined here. The triplet yield of 46 ± 8% for BPh-*a* in acetone/MeOH (7:3 v/v)[27] leaves an internal-conversion yield of approximately 45%.

In contrast to these results, Chl-*a* in diethyl ether has a fluorescence yield of 32%,[28] and a triplet yield of 64%;[29] internal-conversion accounts for only about 4% of the decay. Many other porphyrins have similarly low yields of internal conversion.[30]

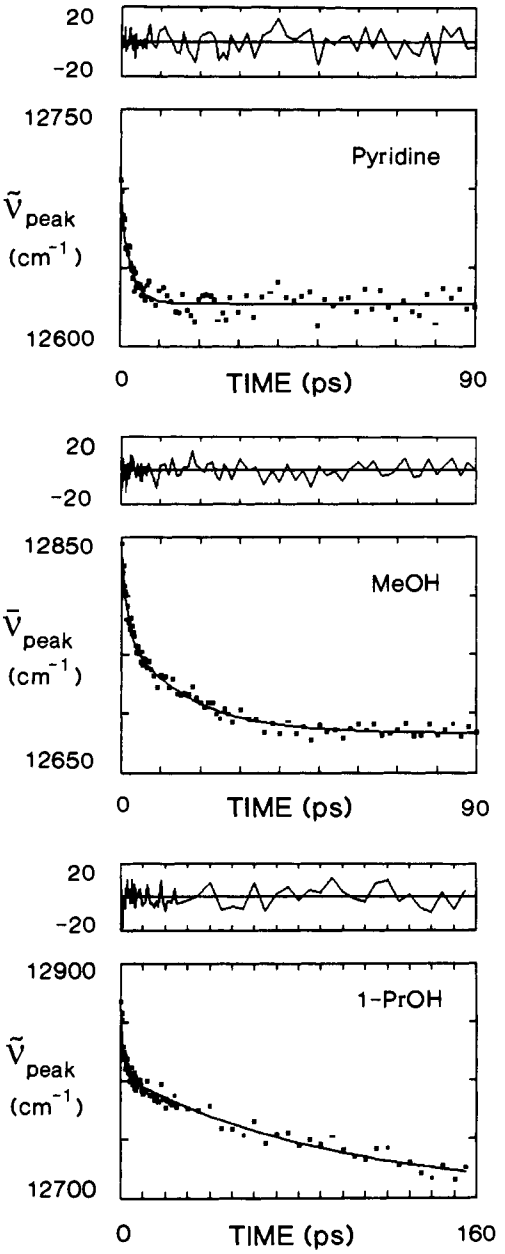

Figure 6. Time dependence of the peaks of the transient difference spectra of BChl in pyridine (a), MeOH (b), and 1-PrOH (c). The positions of the peaks were determined by fitting spectra like those of Figure 5 to a log-normal function (see Methods). The curves through the data are fits to an exponential relaxation with a time constant of 2.7 ps in (a), and to biexponential relaxations with time constants of 1.3 and 16 ps in (b), and 1.3 and 99 ps in (c). The residuals from the fit are shown above each panel.

The importance of internal conversion in BChl may reflect the smaller energy gap between the lowest excited singlet state and the ground state, which results in stronger vibrational wavefunction overlap.[3,31]

Vibronic Coupling and the Breakdown of Mirror Symmetry. As shown in Figure 3, the absorption and emission spectra of BChl-*a* and BPh-*a* violate the mirror-symmetry relationship. The violation is most serious in the vibrational shoulders of the bands, but there is also a deviation in the main part of the spectrum, as is suggested by the different widths of the absorption and emission bands (Table II). Renge et al.,[32] who studied site-selective emission and ex-

(25) Tait, C. D.; Holten, D. *Photochem. Photobiophys.* **1983**, *6*, 201–209.
(26) Gouterman, M.; Holten, D. *Photochem. Photobiol.* **1977**, *25*, 85–92.
(27) Holten, D.; Windsor, M. W.; Parson, W. W.; Gouterman, M. *Photochem. Photobiol.* **1978**, *28*, 951–961.
(28) Weber, G.; Teale, F. W. J. *Trans. Faraday Soc.* **1957**, *53*, 646–655.
(29) Bowers, P. G.; Porter, G. *Proc. R. Soc. London* **1967**, *296*, 435–441.
(30) (a) Harriman, A. *J. Chem. Soc., Faraday Trans. 1* **1980**, *76*, 1978–1985. (b) Kikuchi, K.; Kurabayashi, Y.; Kokubun, H.; Kaizu, Y.; Kobayashi, H. *J. Photochem. Photobiol. A: Chem.* **1988**, *45*, 261–263.
(31) Siebrand, W. *J. Chem. Phys.* **1967**, *46*, 440–447.
(32) Renge, I.; Mauring, K.; Avarmaa, R. *J. Lumin.* **1987**, *37*, 207–214.

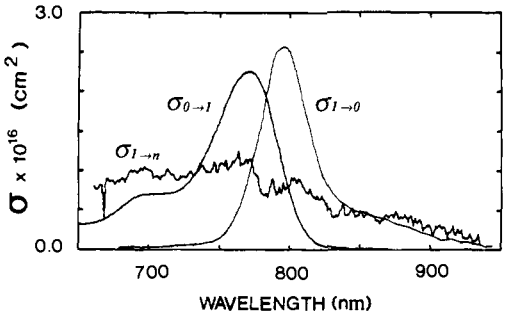

Figure 7. Ground-state absorption spectrum ($\sigma_{0\to1}$), stimulated-emission spectrum ($\sigma_{1\to0}$), and excited-state absorption spectrum ($\sigma_{1\to n}$) of BChl in MeOH. The stimulated-emission spectrum was calculated from the smoothed fluorescence spectrum by eq 17. The excited-state absorption spectrum was obtained by eq 19.

citation spectra of BChl-*a* and BPh-*a* at 4.2 K, concluded that the mirror-symmetry relationship does hold at that temperature. However, they did not obtain data in the vibrational shoulder of the excitation spectrum, where the breakdown of mirror symmetry was most dramatic in the present study. Takiff and Boxer[33] measured absorption and emission spectra of BChl-*a* at 77 K, and their spectra appear to deviate significantly from mirror symmetry in the vibrational shoulders.

The spectra shown in Figure 3 suggest that there is an increase in vibrational energy spacing in the excited state relative to the ground state for one or more of the high-frequency vibrations that underlie the prominent shoulder between the Q_x and Q_y bands in the absorption spectrum. The major vibrational modes with energies in this range include distortions of the methine bridges in the porphyrin ring and C=O stretching of the acetyl and keto groups.[34] Hydrogen bonding to the carbonyl groups evidently is not critical for the breakdown of mirror symmetry, because similar results are obtained in both hydrogen-bonding and non-hydrogen-bonding solvents. The breakdown also appears not to depend strongly on the Mg or its axial ligands, because it occurs with BPh, and with BChl in solvents that provide either one or two ligands (Table I).

A possible cause of the breakdown of mirror symmetry is intensity borrowing between neighboring electronic transitions.[35] In BChl and BPh, it seems likely that one or more of the vibrational modes that underlie the shoulders of the spectra drive a mixing of the Q_x and Q_y excited states. This mixing might be particularly sensitive to the methine vibrations, which perturb the symmetry of the porphyrin ring. Additional evidence for such mixing can be found in the fluorescence polarization spectrum of BChl-*a*. The polarization is near the maximal value of +0.5 when the sample is excited in the main part of the Q_y band, but decreases to about +0.39 in the vibrational shoulder.[36] Variations in polarization also occur across the emission bands of Chl-*a* and Chl-*b*.[37]

Breakdown of the Stepanov Equation by Inhomogeneous Broadening. The fluorescence from BChl-*a* or BPh-*a* does not conform to the Stepanov relationship over the entire emission spectrum; the slope of a plot of eq 9 is lower in the vibrational shoulder than in the main part of the emission band (Figure 4). In addition, the apparent temperature of BChl-*a* or BPh-*a* in the excited state (T^*), as judged from a fit to eq 9 in the central region of the emission spectrum, is higher than the ambient temperature (Table II). Fits that include the vibrational shoulder give larger discrepancies.

Previous investigators have offered a variety of explanations for discrepancies between T^* and the ambient temperature in Chl-*a* and other molecules. These include impurities or aggregation,[10a,b] and lack of attainment of thermal or configurational equilibrium in the excited state.[38] Impurities probably do not account for the elevated T^* in the present case. Although the samples did contain traces of 2-desvinyl-2-acetylchlorophyll-*a* (see Materials), the fits of eq 9 included only spectral regions where fluorescence from this contaminant was negligible. The presence of some BChl-*a*′ and 13²-hydroxy-BChl-*a* probably is not critical in this regard, because the absorption spectra of these materials in the Q_y region are virtually identical with that of BChl-*a*. Aggregation of BChl or BPh does occur in some solvents, but not in the polar, organic solvents used here.[13a] Nor can the results be attributed easily to a departure from thermal equilibrium in the excited state, because excitation into a higher energy band did not increase T^*. Also, the relaxation time constants measured in the picosecond experiments are all much shorter than the fluorescence lifetimes and vary from 2 to 80 ps in the three solvents (Figure 6), whereas the T^* values for BChl-*a* are similar in pyridine, MeOH, and 1-PrOH. Another possible explanation for the discrepancy is a decrease in the fluorescence yield at long wavelengths, where some of the absorption might be due to excitation into higher vibrational levels of the ground state.[10b,38a] Although such excitations might account for part of the weak absorption by BChl-*a* or BPh-*a* at energies below 11 500 cm^{-1} (see Figure 4), they seem unlikely to make an appreciable contribution to the much stronger absorption in the region where we evaluated eq 9.

Perhaps the simplest explanation for the breakdown of the Stepanov relationship is inhomogeneous broadening. Equation 8 says that an individual molecule's fluorescence spectrum is determined uniquely by its absorption spectrum:

$$\frac{F(\tilde{\nu})}{\int F(\tilde{\nu})\,d\tilde{\nu}} = \frac{\tilde{\nu}^2 e^{-\tilde{\nu}/k_BT}\sigma(\tilde{\nu})}{\int \tilde{\nu}^2 e^{-\tilde{\nu}/k_BT}\sigma(\tilde{\nu})\,d\tilde{\nu}} \tag{20}$$

However, the fluorescence from a sample in solution is a superposition of contributions from molecules that interact with the solvent in different ways.[39] Thus, eq 20 becomes

$$\sum_i \left\{F_i(\tilde{\nu}) / \int F_i(\tilde{\nu})\,d\tilde{\nu}\right\} = \tilde{\nu}^2 e^{-\tilde{\nu}/k_BT} \sum_i \sigma_i(\tilde{\nu})/\xi_i \tag{21}$$

where

$$\xi_i = \int \tilde{\nu}^2 e^{-\tilde{\nu}/k_BT}\sigma_i(\tilde{\nu})\,d\tilde{\nu} \tag{22}$$

and subscripts (i) refer to individual molecules. If the absorption spectrum is inhomogeneously broadened, so that ξ_i varies from molecule to molecule, the fluorescence spectrum will be weighted in favor of the molecules that absorb at the highest energies. The value of $\tilde{\nu}_0$ will vary across the absorption and emission spectra, and a plot of ln $[F(\tilde{\nu})/\tilde{\nu}^2\sigma(\tilde{\nu})]$ versus $\tilde{\nu}$ will give a T^* that exceeds the actual temperature of the ensemble.

Radiative Lifetimes and Vibrational Partition Functions. To determine the apparent ratio of the vibrational partition functions of the excited and ground states (Q_g/Q_e) by eq 6, we require a calculated value of the radiative lifetime, τ_0^{calc}. Although τ_0^{calc} can be obtained by eq 4, the results depend on the choice of $\tilde{\nu}_0$. In the present case $\tilde{\nu}_0$ cannot be determined meaningfully from the reflection axis of the absorption and emission spectra or from the intercept of a plot of eq 9 because BChl-*a* and BPh-*a* violate both the mirror-symmetry relationship and eq 9. The estimates of $\tilde{\nu}_0$ obtained by considering only the central regions of the emission

(33) Takiff, L.; Boxer, S. G. *J. Am. Chem. Soc.* **1988**, *110*, 4425–4426.
(34) (a) Cotton, T. M.; Van Duyne, R. P. *J. Am. Chem. Soc.* **1981**, *103*, 6020–6026. (b) Lutz, M. In *Advances in Infrared and Raman Spectroscopy*; Clark, R. J. H., Hester, R. E., Eds.; Wiley-Heyden: London, 1984; Vol. 11, pp 211–300.
(35) (a) Craig, D. P.; Small, G. J. *J. Chem. Phys.* **1969**, *50*, 3827–3834. (b) Perrin, M. H.; Gouterman, M.; Perrin, C. L. *J. Chem. Phys.* **1969**, *50*, 4137–4150. (c) Sharf, B.; Honig, B. *Chem. Phys. Lett.* **1970**, *7*, 132–136. (d) Small, G. J. *J. Chem. Phys.* **1971**, *54*, 3300–3306.
(36) Ebrey, T. G.; Clayton, R. K. *Photochem. Photobiol.* **1969**, *10*, 109–117.
(37) (a) Boxer, S. G.; Kuki, A.; Wright, K. A.; Katz, B. A.; Xuong, N. H. *Proc. Natl. Acad. Sci. U.S.A.* **1982**, *79*, 1121–1125. (b) van Gurp, M.; van Ginkel, G.; Levine, Y. K. *Biochim. Biophys. Acta* **1989**, *973*, 405–413.
(38) (a) Ketskemety, J.; Dombi, J.; Horvai, R. *Acta Phys. Hung.* **1960**, *12*, 263–267. (b) Klochkov, V. P.; Korotkov, S. M. *Opt. Spectrosk. (USSR)* **1967**, *22*, 189–194.
(39) (a) McColgin, W. C.; Marchetti, A. P.; Eberly, J. H. *J. Am. Chem. Soc.* **1978**, *100*, 5622–5626. (b) Stein, A. D.; Fayer, M. D. *Chem. Phys. Lett.* **1991**, *176*, 159–166.

spectra (and neglecting the contribution of ln (Q_g/Q_e) on the right-hand side of eq 9) lead to values of Q_g/Q_e that are somewhat greater than 1.0 (Table I). However, the deviations of the emission spectrum from eq 9 are such that fitting only the central part of the spectrum probably results in an underestimate of the average value of $\tilde{\nu}_0$. Using this value of $\tilde{\nu}_0$ in eq 4 and 6 would lead to an overestimate of Q_g/Q_e. The Strickler–Berg expression (eq 2), on the other hand, assumes at the outset that the nuclear structures of the ground and excited states are similar, and the violation of mirror symmetry is presumptive evidence that this assumption has broken down. The calculated radiative lifetimes and ratios of partition functions give values of Q_g/Q_e that are somewhat below 1.0 (Table I).

Taken together, these results indicate that Q_g/Q_e is probably close to 1.0, with an uncertainty on the order of ±0.3. This may appear to conflict with the conclusion that the excitation of BChl-*a* causes increases in the frequencies of vibrational modes that underlie the shoulders of the absorption and emission spectra. However, changes in these high-frequency modes would have relatively small effects on the partition function, because of the exponential falloff of their contributions with energy (eq 5).

Picosecond Dynamics of Excited BChl. The transient difference spectra measured in the picosecond experiments (Figure 5) are characterized by a sharp trough on the red side of the Q_y absorption band and a broad absorbance increase at shorter wavelengths. These features reflect bleaching of the ground-state spectrum, stimulated emission, and excited-state absorption. Because the fluorescence lifetime is on the order of 2.5 ns,[3] triplet states and unrelaxed ground states created by the decay of the excited state are unlikely to contribute significantly to the spectra. Though some porphyrins with open-shell metals release or bind axial ligands when they are excited,[40] such effects are probably not important here because BChl has a closed-shell metal atom that is relatively unreactive. Finally, there is no evidence for photooxidation of the BChl, because no absorption bands are seen near 850–950 nm, where the BChl radical cation[41a] and solvated electrons in alcohols[41b] absorb.

Time-dependent shifting of the stimulated emission could reflect intramolecular vibrational relaxation (redistribution of energy from excited vibronic modes to other modes), vibrational cooling (transfer of energy to the solvent), or dielectric relaxation of the solvent (rotational reorientation of solvent molecules around the excited BChl). Because the relaxation time constants that we measured depend strongly on the solvent, they probably reflect dielectric relaxation and/or vibrational cooling, rather than a purely intramolecular process. Rodriguez and Holten[40b,42] have used picosecond absorption spectroscopy to study excited Ni porphyrins in nonpolar solvents. They measured a time constant of about 20 ps for recovery of ground-state absorption, which they attributed mostly to vibrational cooling with possible contributions from intramolecular vibrational relaxation. Other investigators studying the shifting of the absorption or spontaneous fluorescence spectra of a variety of dye molecules have described relaxations ranging from <1 to about 100 ps, and have attributed the dynamics mainly to dielectric relaxation of the solvent.[43] The kinetics are usually multiphasic. In nonviscous, polar, aprotic solvents at room temperature, the relaxation typically occurs in 4 ps or less.[43d,e] In MeOH, time constants of 3.3 ps,[43f] 1.2 and 9 ps,[43e] 0.8 and 20 ps,[43g] and 1.4 and 10.9 ps[43j] have been observed. Time constants of about 100 ps,[43h] 17 and 100 ps,[43f] and <30 ps and 60 ps[43i] have been observed in 1-PrOH and similar long-chain alcohols. Our results agree well with the time constants measured in these studies.

Most of the theoretical treatments that have been applied to the electron-transfer kinetics in RCs have assumed that the excited BChl dimer reaches thermal equilibrium rapidly relative to the rate of electron transfer. In RCs of *Rb. sphaeroides*, where electron transfer proceeds in about 3.5 ps, no relaxations were observed in the stimulated-emission spectrum.[2c] The different behavior of excited BChl in the RC compared to solution can be attributed plausibly to the more rigid surroundings provided by the protein, which limit the amount of reorganization that can occur. However, in RCs of *Chloroflexus aurantiacus*, where electron transfer takes about 7 ps, there are indications of a small shift of the stimulated-emission spectrum during the first 1.5 ps after excitation.[18] Shifts of the emission to *shorter* wavelengths have been detected in RCs of mutant bacterial strains in which electron transfer is retarded.[2e]

Absorption Spectrum of Excited BChl. Although there is little information in the literature on $S_1 \rightarrow_n$ absorption in BChl-*a*, the excited singlet state of Chl-*a* appears to have a broad absorption band in the red region of the spectrum.[44] However, considerable uncertainty has remained in the value of $\sigma_{1\rightarrow n}$ for Chl-*a*, largely because of the difficulties of determining the fraction of the molecules that are in the excited state and of distinguishing absorbance changes from stimulated emission. For BChl-*a*, the only relevant study appears to be that of Hindman et al.,[44f] who measured fluorescence spectra and relative fluorescence yields for BChl-*a* as a function of detection geometry, using high-intensity laser excitation. They concluded that BChl-*a* has significant $S_1 \rightarrow_n$ absorption in the region of the Q_y band, but they did not estimate $\sigma_{1\rightarrow n}$ quantitatively.

To obtain the $S_1 \rightarrow_n$ absorption spectrum of BChl-*a*, we determined the fraction of excited molecules by using RCs as an actinometer. Contributions of stimulated emission were evaluated by calculating the stimulated-emission spectrum from the steady-state absorption and fluorescence spectra and the measured fluorescence yield and lifetime. The broad $S_1 \rightarrow_n$ absorption spectrum of BChl-*a* has an integrated area comparable to the area of the ground state's strong Q_y absorption band (Figure 7). Similar spectra could contribute to the transient signals associated with the excited states of RCs and BChl-protein antenna complexes.

Acknowledgment. We are indebted to G. Hartwich in the laboratory of Professor H. Scheer for help with the HPLC measurements, M. Shield and D. Middendorf for help with some of the computer programming, O. Oleinik and M. Larvie for preparing RCs, and B. S. Fujimoto, M. Gouterman, D. Holten, R. T. Ross, and J. M. Schurr for helpful discussions. This work was supported by NSF Grant PCM-8616563.

Registry No. Bacteriochlorophyll *a*, 17499-98-8; bacteriopheophytin *a*, 17453-58-6.

(40) (a) Holten, D.; Gouterman, M. In *Optical Properties and Structure of Tetrapyrroles*; Blauer, G., Sund, H., Eds.; Walter de Gruyter: New York, 1985; pp 63–90. (b) Rodriguez, J.; Holten, D. *J. Chem. Phys.* **1990**, *92*, 5944–5950.

(41) (a) Fajer, J.; Borg, D. C.; Forman, A.; Felton, R. H.; Dolphin, D.; Vegh, L. *Proc. Natl. Acad. Sci. U.S.A.* **1974**, *71*, 994–998. (b) Chase, W. J.; Hunt, J. *J. Phys. Chem.* **1975**, *79*, 2835–2845.

(42) Rodriguez, J.; Holten, D. *J. Chem. Phys.* **1989**, *91*, 3525–3531.

(43) (a) Fleming, G. R. *Chemical Applications of Ultrafast Spectroscopy*; Oxford University Press: New York, 1986. (b) Simon, J. D. *Acc. Chem. Res.* **1988**, *21*, 128–134. (c) Barbara, P. F.; Jarzeba, W. *Adv. Photochem.* **1990**, *19*, 1–68. (d) Jarzeba, W.; Walker, G. C.; Johnson, A. E.; Kahlow, M. A.; Barbara, P. F. *J. Phys. Chem.* **1988**, *92*, 7039–7041. (e) Kahlow, M. A.; Jarzeba, W.; Kang, T. J.; Barbara, P. F. *J. Chem. Phys.* **1989**, *90*, 151–158. (f) Castner, E. W., Jr.; Maroncelli, M.; Fleming, G. R. *J. Chem. Phys.* **1987**, *86*, 1090–1097. (g) Mokhtari, A.; Chesnoy, J.; Laubereau, A. *Chem. Phys. Lett.* **1989**, *155*, 593–598. (h) Declémy, A.; Rullière, C.; Kottis, Ph. *Chem. Phys. Lett.* **1987**, *133*, 448–454. (i) Maroncelli, M.; Fleming, G. R. *J. Chem. Phys.* **1987**, *86*, 6221–6239. (j) Ernsting, N. P.; Kaschke, M. *Rev. Sci. Instrum.* **1991**, *62*, 600–608.

(44) (a) Arsenault, R.; Denariez-Roberge, M. M. *Chem. Phys. Lett.* **1976**, *40*, 84–87. (b) Huppert, D.; Rentzepis, P. M.; Tollin, G. *Biochim. Biophys. Acta* **1976**, *440*, 356–364. (c) Leupold, D.; Mory, S.; König, R.; Hoffman, P.; Hieke, B. *Chem. Phys. Lett.* **1977**, *45*, 567–571. (d) Leupold, D.; Ehlert, J.; Oberländer, S.; Wiesner, B. *Chem. Phys. Lett.* **1983**, *100*, 345–350. (e) Leupold, D.; Scholz, M.; Ehlert, J. *Chem. Phys. Lett.* **1985**, *115*, 434–436. (f) Hindman, J. C.; Kugel, R.; Svirmickas, A.; Katz, J. J. *Chem. Phys. Lett.* **1978**, *53*, 197–200. (g) Baugher, J.; Hindman, J. C.; Katz, J. J. *Chem. Phys. Lett.* **1979**, *63*, 159–162. (h) Shepanski, J. F.; Anderson, R. W., Jr. *Chem. Phys. Lett.* **1981**, *78*, 165–173. (i) Hunt, J. E.; Katz, J. J.; Svirmickas, A.; Hindman, J. C. *Chem. Phys.* **1983**, *82*, 413–426. (j) Koningstein, J. A. *J. Raman. Spectrosc.* **1989**, *20*, 83–90.